Analytical Procedure for Calculation of Attached and Separated Subsonic Diffuser Flows

William W. Bower*
McDonnell Aircraft Company, St. Louis, Mo.

An analytical procedure for computing the static and total pressure distributions in subsonic diffusers with axisymmetric or two-dimensional cross sections is described. It includes velocity profile and shear stress parameters which apply to attached and separated flows and allows for a strong interaction between the inviscid and viscous portions of the duct flow. With this approach, solutions can be obtained for separated regions where conventional boundary-layer methods fail. Analytical and experimental static and total pressure distributions are compared for plane-wall and conical diffusers. An approximate technique is used to apply the analysis to actual aircraft diffusers.

Nomenclature

A = geometric cross-sectional area of diffuser
A_e = effective flow cross-sectional area of diffuser
a_0 = speed of sound based on freestream stagnation temperature
$a_1,\ldots,a_7$ = coefficients appearing in axisymmetric integral boundary-layer equations
b_1,b_2,b_3 = coefficients appearing in the axisymmetric integral boundary-layer equations
C_D = shear work integral
D = diameter of diffuser exit plane
d = diameter of diffuser entrance plane
f = dimensionless transformed momentum thickness variable
H = physical boundary-layer shape factor, δ^*/θ
H_{tr} = transformed boundary-layer shape factor, Δ^*/Θ
$\bar{H}_{tr}$ = transformed boundary-layer energy thickness factor, Δ^{**}/Θ
h = local height for two-dimensional diffuser cross section
h_1 = entrance plane height for two-dimensional diffuser
J = boundary-layer profile parameter, $\bar{H}_{tr}/H_{tr}$
L = total diffuser length
M = Mach number
M_e = Mach number at edge of boundary layer
$P_{T,AVE}$ = area-averaged total pressure
$(P_{T,CORE})_1$ = diffuser entrance-plane core stagnation pressure
P_W = wall static pressure
P = static pressure
R = axisymmetric body radius
Re_Δ = Reynolds number based on transformed boundary-layer thickness
s = surface coordinate in boundary-layer system of coordinates
$\bar{s}$ = transformed surface coordinate in boundary-layer system of coordinates
T_e = static temperature at edge of boundary layer
T_0 = freestream stagnation temperature
$(T_{T,CORE})_1$ = diffuser entrance plane core stagnation temperature
T_w = wall temperature
$\bar{T}$ = reference temperature
U = transformed longitudinal velocity
U_e = transformed longitudinal velocity at edge of boundary layer
u = physical longitudinal velocity
w = local width for two-dimensional diffuser cross section
w_1 = entrance plane width for two-dimensional diffuser
x = diffuser axial coordinate
γ = ratio of specific heat capacities, 1.4
Δ = transformed boundary-layer thickness
Δ^* = transformed boundary-layer displacement thickness,

$$\Delta^* \equiv \int_0^\Delta (1 - \frac{U}{U_e})\, d\bar{\eta}$$

Δ^{**} = transformed boundary-layer energy-loss thickness,

$$\Delta^{**} \equiv \int_0^\Delta \frac{U}{U_e}(1 - \frac{U^2}{U_e^2})\, d\bar{\eta}$$

δ = physical boundary-layer thickness
δ^* = physical boundary-layer displacement thickness,

$$\delta^* \equiv \int_0^\delta (1 - \frac{\rho u}{\rho_e u_e})\, dy$$

δ^*_p = projection of δ^* normal to x
η = normal coordinate in boundary-layer system of coordinates
$\bar{\eta}$ = transformed normal coordinate in boundary-layer system of coordinates
Θ = transformed boundary-layer momentum thickness,

$$\Theta \equiv \int_0^\Delta \frac{U}{U_e}(1 - \frac{U}{U_e})\, d\bar{\eta}$$

θ = physical boundary-layer momentum thickness,

$$\theta \equiv \int_0^\delta \frac{\rho u}{\rho_e u_e}(1 - \frac{u}{u_e})\, dy$$

θ_w = one-half diffuser included divergence angle

Received March 10, 1975.
Index categories: Jets, Wakes, and Viscid-Inviscid Flow Interactions; Airbreathing Propulsion, Subsonic and Supersonic.

*Senior Engineer, Propulsion. Now Research Scientist, McDonnell Douglas Research Laboratories, St. Louis, Mo. Member AIAA.

μ_0 = molecular viscosity based on stagnation conditions
$\bar{\mu}$ = molecular viscosity based on reference conditions
ν_0 = kinematic viscosity based on stagnation conditions
ρ = mass density
ρ_e = static density at edge of boundary layer
ρ_0 = freestream stagnation density

Introduction

A HIGH-performance air induction system for an aircraft requires a well-designed subsonic diffuser to ensure that the engine receives the required airflow at high total pressure and with acceptable distortion. The principal design problem is to define the duct geometry that will provide the highest performance for given airframe constraints and diffuser entrance conditions.

Currently, the problem is solved almost solely by using empirical data. Performance maps or empirical correlation procedures are used to determine the variation in total pressure recovery, distortion, and turbulence with diffuser length, area ratio, average entrance Mach number, and entrance boundary-layer blockage. These data are used to select a promising configuration, and then the actual diffuser performance is determined through model testing.

Although this approach can provide high-recovery, low-distortion diffusers, it has certain shortcomings. Many of the available diffuser performance maps and correlations provide only static pressure recovery. Total pressure recovery and distortion are not given. In addition, the ranges and combinations of entrance conditions and geometric variables for which data are available are extremely limited.

Consequently, the need exists for a generalized procedure which can be used to estimate subsonic diffuser performance for all possible combinations of entrance conditions and for any arbitrary configuration. The latter includes long, high-volume ducts and short, low-volume ducts with any degree of curvature and any cross-sectional shape. In addition, rather than simply providing performance values, it would be desirable for the procedure to provide insight into why a candidate diffuser configuration may have poor performance and what geometry corrections can be made to improve it. These requirements for complete generality and, at the same time, for details of the local flowfield indicate the need for an analytical rather than an empirical correlation procedure.

In this paper an analytical technique for calculating the boundary-layer characteristics and the static and total pressure distributions in plane-wall and conical diffusers is defined. It is the first step toward developing a procedure to predict the performance of subsonic diffusers with arbitrary entrance conditions and geometry. The present technique is applicable to compressible turbulent flows with or without boundary-layer separation. The development of the viscous and inviscid equations is discussed, along with the manner in which they are coupled. Representative comparisons between predicted and measured flowfield data for both plane-wall and conical diffusers are presented for a variety of diffuser geometries and operating conditions. Results are also shown for cases in which the analytical model was used in an approximate manner to predict the flow in actual aircraft diffuser configurations for which the cross sections vary from two-dimensional to circular. Conclusions are drawn regarding the accuracy and usefulness of the model.

Definition of the Problem

In the past decade numerous analytical techniques have been developed for computing internal viscous flows. However, for these to be of general use in aircraft propulsion applications, they must apply to compressible turbulent flows

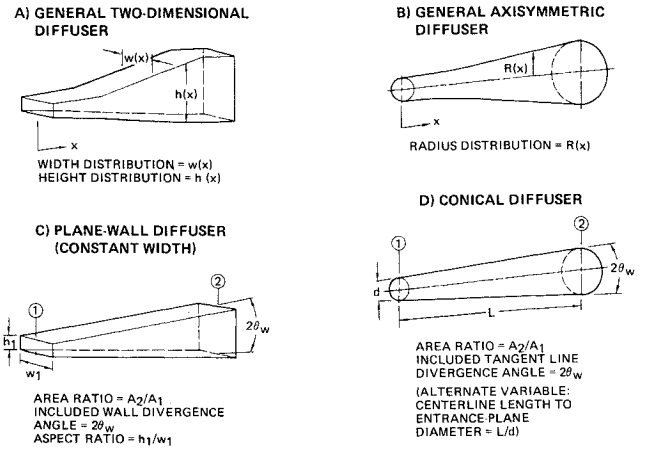

Fig. 1 Representative subsonic diffuser configurations.

and permit the calculation of regions of boundary-layer separation, which are frequently unavoidable in short, low-volume ducts that have relatively large diffusion rates. When these requirements are considered, the number of available analytical techniques is reduced to one,[1] and this procedure can provide only limited performance predictions.

The technique discussed in this paper provides both the static and total pressure distributions in a subsonic diffuser. It applies directly to diffusers with rectangular or circular cross sections, as shown in Fig. 1.

Physical Considerations

Even for simple geometries, the flow patterns in a subsonic diffuser can be quite complex. As pointed out by Reneau et al.,[2] flow visualization reveals various types of boundary-layer separation with drastically different characteristics. The separated zone may be quasi-steady in character and envelop the entire circumference of the diffuser, constricting the inviscid core flow to a jet (jet-flow regime), or it may be unsteady, varying in position, size, and intensity (transitory stall). Thus, the separated region may have an influence on the entire cross-sectional area of the diffuser or on only localized regions, such as corners.

Frequently, the unsteady character of the separated flow in a subsonic diffuser causes a significant propulsion system problem through time-variant distortion. Currently, the analysis of unsteady three-dimensional viscous duct flows is beyond the scope of computationally rapid techniques which can be used in subsonic diffuser design studies. For this reason, this paper deals solely with the problem of computing the steady-state flow. With this approach, the boundary layer may remain attached the entire duct length, may separate and remain detached, or may reattach at some point downstream.

Analytical Considerations

The major obstacle in analytically predicting the flow in subsonic diffusers is the method of treating the region of boundary-layer separation. In the absence of a solution of the complete Navier-Stokes equations and with the failure of conventional marching-type internal-flow techniques, there is currently a need for approximate prediction procedures.

Although these analytical models may be gross simplifications of the real unsteady, three-dimensional separated diffuser flow, they seem to be warranted in lieu of relying solely on experiment for diffuser design and analysis until computerized solutions of the Navier-Stokes equations become feasible.

The analytical model described here is applicable to both compressible and incompressible turbulent subsonic diffuser flows, with or without boundary-layer separation. The technique, which is referred to as "strong interaction

theory," is an adaptation to internal flow of the concepts developed by Klineberg and Steger[3] for the calculation of external subsonic and transonic separated flows.

Strong interaction theory is best understood by assessing the limitations of weak interaction theory, which is the standard boundary-layer approach for analyzing an attached diffuser flow. With this technique the boundary layer is assumed to be extremely thin and therefore only weakly coupled to the inviscid core. As a result, the pressure distribution computed for the actual geometry does not differ significantly from the distribution computed for the effective inviscid geometry (the actual corrected by the boundary-layer displacement thickness). Consequently, the inviscid pressure distribution can be imposed on a system of boundary-layer equations to obtain a physically realistic variation in displacement thickness along the diffuser. This permits the calculation of a new effective inviscid geometry and associated pressure distribution, and after several cyclic iterations the solution converges.

The characteristics of separated flow prevent the use of weak interaction theory. As the boundary layer approaches separation, the displacement thickness increases to the extent that the pressure distribution computed for the effective inviscid core area differs significantly from that computed for the actual geometric area of the diffuser. This means that, in the vicinity of separation, an inviscid pressure distribution cannot be imposed on the viscous equations, as in weak interaction theory. If this is done, the boundary-layer parameters diverge, and a physically realistic solution is not possible. Rather, the pressure distribution and viscous parameters must be computed simultaneously, which is the essence of strong interaction theory.

The strong interaction model for a subsonic diffuser is based on a one-dimensional description of the inviscid region and solves in differential form the compressible isentropic flow conservation equations for the core simultaneously with a system of integral equations for the turbulent compressible viscous layer. For two-dimensional diffusers, boundary-layer growth on all four walls is taken into account. The backflow characteristics are included through use of an appropriate velocity profile and shear-work-integral variation, which is based on experimental data for both attached and separated boundary layers. Through use of the one-dimensional core flow approximation and the integral description of the boundary layer, the entire problem can be carried out stepwise along the diffuser using a Runge-Kutta integration scheme. A marching solution is possible, even when reverse flow exists, since integral parameters are computed which describe the boundary layer as a whole, not the velocity field. The boundary-layer solution is then carried out in the dominant flow direction that characterizes the entire layer, and this is the direction of the mainstream.

Development of Strong Interaction Solution Procedure

The analytical model for predicting the flow in a subsonic diffuser is based on the coupled solution of a system of equations describing the viscous layer and a system describing the inviscid core.

Viscous Equations

The Prandtl boundary-layer equations for steady, compressible turbulent flow are the starting point of the mathematical model of the viscous layer. Conservation of energy is imposed through the constraint that the total temperature must remain constant throughout the diffuser.

To write the equations in an incompressible form, a Mager-type compressibility transformation[4] is introduced in which the transformed boundary-layer coordinates ($\bar{s}$, $\bar{\eta}$) become the independent variables. For simplicity, the resulting differential equations are solved in integral form. The first of the two integral equations, the momentum integral equation, is

$$\frac{d\Theta}{d\bar{s}} + (H_{tr}+2)\frac{\Theta}{U_e}\frac{dU_e}{d\bar{s}} + \frac{\Theta}{R}\frac{dR}{d\bar{s}} = \left(\frac{\bar{T}}{T_e}\right)\frac{\tau_w}{\rho_e U_e^2} \quad (1)$$

and the second, the transformed velocity moment equation, is

$$\Theta\frac{d\bar{H}_{tr}}{d\bar{s}} = (H_{tr}-1)\frac{\bar{H}_{tr}\Theta}{U_e}\frac{dU_e}{d\bar{s}} + \left(\frac{\bar{T}}{T_e}\right)\frac{2}{\rho_e U_e^2} \times \int_0^{\Delta}\tau\frac{\partial}{\partial\bar{\eta}}\left(\frac{U}{U_e}\right)d\bar{\eta} - \left(\frac{\bar{T}}{T_e}\right)\bar{H}_{tr}\frac{\tau_w}{\rho_e U_e^2} \quad (2)$$

For a two-dimensional (planar) flow, $R=1$, while for an axisymmetric flow, $R=R(s)$, a specified function of the surface coordinate. The transformed integral boundary-layer parameters which appear in these equations are the momentum thickness Θ, the shape factor H_{tr}, and the energy thickness factor $\bar{H}_{tr}$. The momentum integral and velocity moment equations contain the following seven unknowns:

$$\frac{\bar{T}}{T_e},\ \frac{\tau_w}{\rho_e U_e^2},\ \frac{2}{\rho_e U_e^2}\int_0^{\Delta}\tau\frac{\partial}{\partial\bar{\eta}}\left(\frac{U}{U_e}\right)d\bar{\eta},$$

$$\bar{H}_{tr},\ H_{tr},\ \Theta,\text{ and } U_e$$

but the first four can be directly related to the last three. $\bar{T}/T_e$ is evaluated from the reference temperature relation of Ref. 4 and the defining equation for the stagnation temperature once U_e is known. The wall shear term $\tau_w/\rho_e U_e^2$ is related to the remaining variables through an extension of the Ludwieg-Tillman skin-friction coefficient to compressible flow[4,5]

$$\frac{\tau_w}{\rho_e U_e^2} = 0.123e^{-1.561H_{tr}}\left(\frac{U_e\Theta}{\nu_0}\right)^{-0.268} \times \left(\frac{T_e}{T_o}\right)\left(\frac{T_e}{\bar{T}}\right)\left(\frac{\bar{\mu}}{\mu_0}\right)^{0.268} \quad (3)$$

The Ludwieg-Tillman skin-friction coefficient does not provide a negative wall shear stress for values of the transformed shape factor which are indicative of boundary-layer separation. However, a more accurate relation based on measurements in separated boundary layers is not available. Therefore, in the present analysis it is assumed that the wall shear stress is negligible, compared with the maximum turbulent stress in the spearated boundary layer. Equation (3) does provide a vanishing τ_w with increasing H_{tr}.

The shear work integral

$$\frac{2}{\rho_e U_e^2}\int_0^{\Delta}\tau\frac{\partial}{\partial\bar{\eta}}\left(\frac{U}{U_e}\right)d\bar{\eta}$$

can be written as

$$\frac{2}{\rho_e U_e^2}\int_0^{\Delta}\tau\frac{\partial}{\partial\bar{\eta}}\left(\frac{U}{U_e}\right)d\bar{\eta} = \left(\frac{T_e}{T_0}\right)C_D \quad (4)$$

where

$$C_D = \frac{2}{\rho_e u_e^3}\int_0^{\delta}\tau\frac{\partial u}{\partial y}\,dy$$

and is evaluated from a curve fit to the experimental values of C_D compiled by Alber[6] for both attached and separated flows. The boundary-layer shape and energy thickness factors H_{tr} and $\bar{H}_{tr}$ are related through their definitions. At this point

in the analysis it is necessary, for the first time, to assume a form of the velocity profile. To introduce a realistic representation of the velocity profile for both an attached and separated boundary layer, a modified form of the Coles profile developed by Escudier and Nicoll[7] is used in the analysis.

$$\frac{U}{U_e} = \left[\frac{3-H_{tr}}{2H_{tr}}\right][1+\ell n\,(\bar{\eta}/\Delta)/\ell n\,(0.565Re_\Delta)]$$

$$+\tfrac{3}{4}\left[\frac{H_{tr}-1}{H_{tr}}\right][1-\cos(\pi\bar{\eta}/\Delta)] \qquad (5)$$

where Re_Δ is the Reynolds number based on the transformed boundary-layer thickness. Figure 2 shows the modified Coles profile as a function of H_{tr}.

Escudier and Nicoll[7] have shown that the relationship between $\bar{H}_{tr}$ and H_{tr} for the Coles profile can be represented by

$$\bar{H}_{tr} = 1.431 - (0.0971/H_{tr}) + (0.775/H_{tr}^2) \qquad (6)$$

which is the expression used in the present analysis. For computational purposes Eqs. (1) and (2) are rewritten, relating the transformed velocity U_e to the Mach number M_e, and introducing the boundary-layer profile parameter J and a dimensionless transformed momentum thickness variable[4]

$$f = (M_e a_0 \Theta/\nu_0)^{1.268}$$

Derivatives with respect to the transformed coordinate $\bar{s}$ are expressed in terms of the physical coordinate s using the compressibility transformation.

With these changes Eqs. (1) and (2) take the following form:

$$\frac{df}{ds} + 1.268f(H_{tr}+1)\frac{d\ell nM_e}{ds} = -1.268\frac{f}{R}\frac{dR}{ds} + 1.268\lambda \qquad (7)$$

$$\left(\frac{1}{H_{tr}} + \frac{1}{J}\frac{dJ}{dH_{tr}}\right)\frac{dH_{tr}}{ds} - (H_{tr}-1)\frac{d\ell nM_e}{ds}$$

$$= \frac{1}{JH_{tr}}\left(\frac{M_e a_0}{\nu_0}\right)f^{-0.78864}\left(\frac{T_e}{T_0}\right)^3 C_D - \frac{\lambda}{f} \qquad (8)$$

where

$$\lambda = 0.123e^{-1.561H_{tr}}\left(\frac{M_e a_0}{\nu_0}\right)\left(\frac{T_e}{\bar{T}}\right)\left(\frac{T_e}{T_0}\right)^3\left(\frac{\mu}{\mu_0}\right)^{0.268} \qquad (9)$$

Viscous-Inviscid Coupling

The Mach number variation in the diffuser can be related to the area change through the differential form of the continuity equation for one-dimensional isentropic flow

$$\frac{1}{A}\frac{dA}{dx} + \left[1 - \frac{(\gamma+1)M^2}{2[1+\tfrac{1}{2}(\gamma-1)M^2]}\right]\frac{d\ell nM}{dx} = 0 \qquad (10)$$

Axisymmetric Diffuser

Consider, first, the simpler case of an axisymmetric diffuser for which the radius distribution $R(x)$ is specified. The effective inviscid flow area at any axial station is given by

$$A_e(x) = \pi[R(x) - \delta^*_p(x)]^2 \qquad (11)$$

$$\frac{U}{U_e} = Z\left\{1 + [\ell n\,(\bar{\eta}/\Delta)]/\ell\right\} + \tfrac{1}{2}(1-Z)\,w\,(\bar{\eta}/\Delta)$$

$$Z = \frac{3-H_{tr}}{2\,H_{tr}}$$

$$\ell = \ell n\,(0.565\,Re_\Delta)$$

$$w = 1 - \cos(\pi\,\bar{\eta}/\Delta)$$

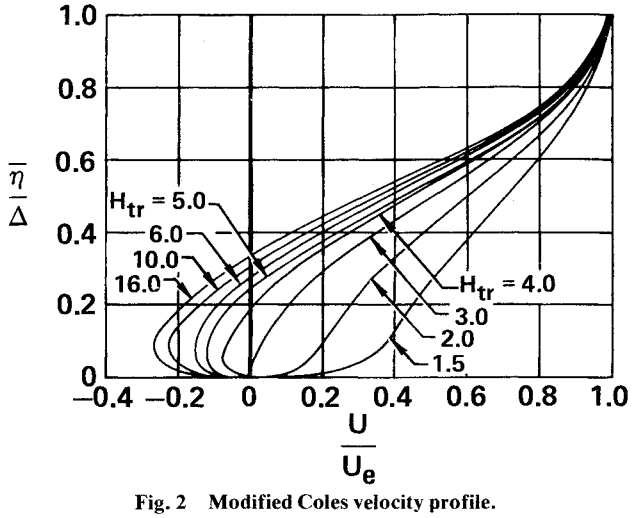

Fig. 2 Modified Coles velocity profile.

The projection of δ^* normal to x, δ^*_p, is approximated by δ^*, and substitution of Eq. (11) into Eq. (10) results in

$$\frac{dR}{dx} - \frac{d\delta^*}{dx} + \tfrac{1}{2}(R-\delta^*)\left\{1 - \frac{(\gamma+1)M^2}{2[1+\tfrac{1}{2}(\gamma-1)M^2]}\right\} \times \frac{d\ell nM}{dx} = 0 \qquad (12)$$

Through the compressibility transformation used in the boundary-layer equations, the physical displacement thickness appearing in Eq. (12) can be directly related to the transformed displacement and momentum thicknesses. In the boundary-layer equations the independent variable can be changed from s to x through

$$d(\,)/ds = [d(\,)/dx]\;dx/ds$$

With these substitutions, the equations for the viscous and inviscid regions of the flow take the following matrix form:

$$\begin{bmatrix} a_1 & a_2 & a_3 \\ 0 & a_6 & a_7 \\ a_4 & 0 & a_5 \end{bmatrix}\begin{bmatrix} \frac{df}{dx} \\ \frac{dH_{tr}}{dx} \\ \frac{d\ell nM_e}{dx} \end{bmatrix} = \begin{bmatrix} b_1 \\ b_3 \\ b_2 \end{bmatrix} \qquad (13)$$

The a and b coefficients are functions of the unknown variables and the diffuser geometry. Starting with the values of δ^*, H_{tr}, and M_e (and thereby f) specified at the diffuser entrance plane, Eq. (13) is solved stepwise along the diffuser for f, H_{tr}, and M_e, using a fourth-order Runge-Kutta integration scheme.

Two-Dimensional Diffuser

Now consider the case of a two-dimensional diffuser for which a height variation $h(x)$ and width variation $w(x)$ are specified. Using the notation 1, 2, 3, and 4 to denote the up-

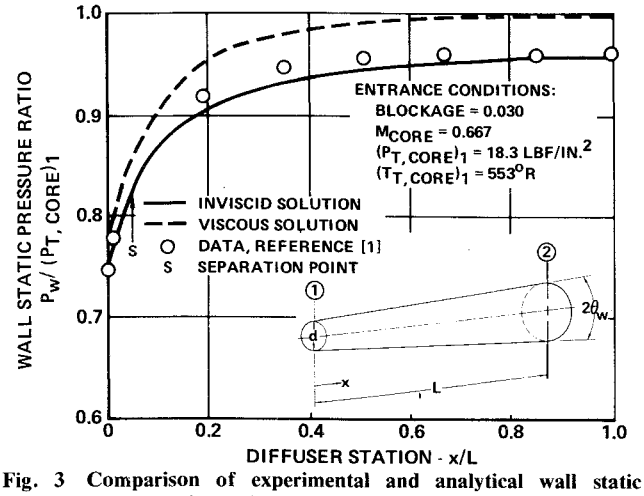

Fig. 3 Comparison of experimental and analytical wall static pressure distributions (conical diffuser with $A_2/A_1 = 9.14$, $2\theta_w = 8.09°$, and $L/d = 15.49$).

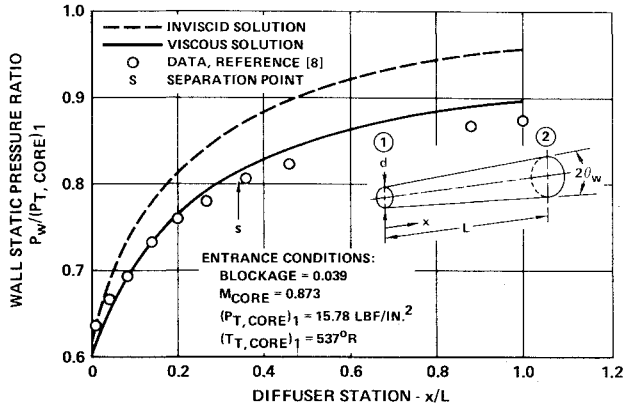

Fig. 4 Comparison of experimental and analytical wall static pressure distributions (conical diffuser with $A_2/A_1 = 2.43$, $2\theta_w = 4°$, and $L/d = 8$).

per, lower, right, and left diffuser walls, respectively, the effective inviscid flow area for the diffuser is given by

$$A_e(x) = [h(x) - \delta^*_{1,p}(x) - \delta^*_{2,p}(x)] \times [w(x) - \delta^*_{3,p}(x) - \delta^*_{4,p}(x)] \quad (14)$$

A matrix equation analogous to Eq. (13) can be derived for a two-dimensional diffuser by combining Eqs. (10) and (14) and following the same steps as used in the analysis for the axisymmetric case. However, for the two-dimensional diffuser, there are two boundary-layer equations for each surface, which must be coupled to the core-flow equation, so the resulting matrix is 9×9. It, too, is solved with Runge-Kutta integration, starting with the entrance plane conditions.

Sample Problem Solution

To establish the accuracy of the present analytical scheme, the technique was applied to a variety of diffuser configurations and operating conditions for which experimental performance measurements are available.

Axisymmetric Diffuser Solutions

Data used to examine the accuracy of the analytical procedure for axisymmetric ducts were obtained from four different experimental investigations of conical diffusers. Details of the configurations and test conditions are described in Refs. 1-10.

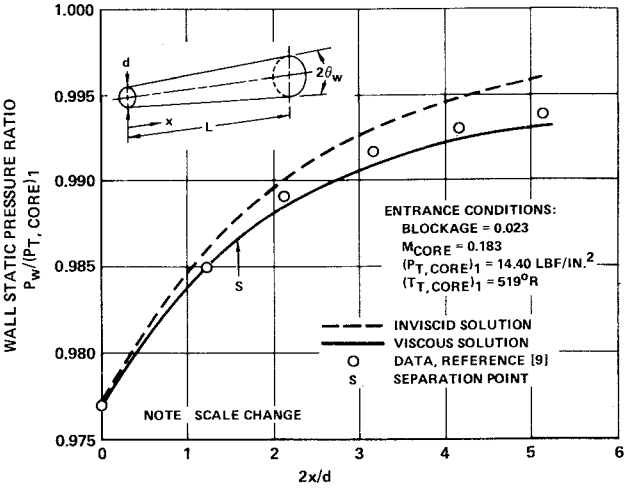

Fig. 5 Comparison of experimental and analytical wall static pressure distributions (conical duffuser with $A_2/A_1 = 2.43$, $2\theta_w = 12.02°$, and $L/d = 2.671$).

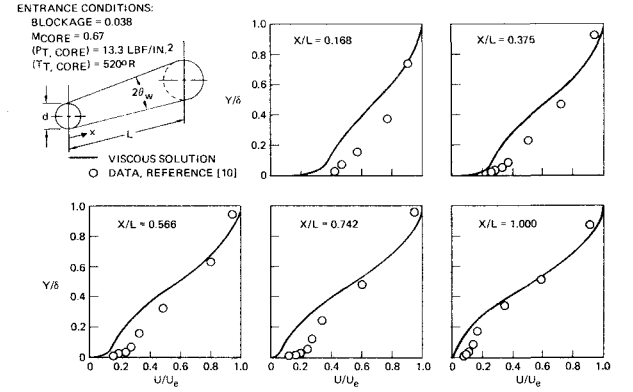

Fig. 6 Comparison of experimental and analytical boundary-layer velocity profiles (conical diffuser with $A_2/A_1 = 2.0$, $2\theta_w = 12°$, and $L/d = 2.0$).

Representative distributions of the ratio of wall static pressure to the entrance core stagnation pressure are shown in Figs. 3-5 for different data sources. The inviscid solutions were computed using one-dimensional compressible-flow theory, and the viscous solutions were obtained using the present analytical model with the entrance conditions listed on each figure. Approximately a quarter minute of CDC 6600 central processing time was required for each solution.

To determine whether a given subsonic diffuser flow is separated, it is necessary to select a criterion based on the computed integral boundary-layer parameters. As Fig. 2 illustrates, the modified Coles profile is representative of an attached flow for $H_{tr} < 3$. It should be noted that a power-law profile, on which most integral boundary-layer theories are based, is also representative of an attached-flow profile for $H_{tr} \leq 3$. However, experimental measurements have shown that boundary-layer separation can occur for a value of H_{tr} as low as 1.8 or can be delayed until a value as high as 3.6 is reached. In the present work a conservative approach is adopted, and the indicated separation points were determined on the basis of a transformed shape factor of 1.8.

Boundary-layer velocity profile data are available from the conical diffuser test program described in Ref. 10. Figure 6 shows a comparison of the experimental and analytical velocity distributions at various locations in the duct. It should be noted that, in the experimental evaluation of the ratio of the local velocity in the boundary layer to the velocity at the edge, an incompressible-flow equation was used to relate the velocity ratio to the measured static total pressures.

Of the four data sources for conical diffusers, only Refs. 9 and 10 contain total pressure losses. Figure 7 illustrates the

ENTRANCE CONDITIONS:

B	0.038	0.038	0.038	0.038	0.038	
M_{CORE}	0.790	0.765	0.670	0.530	0.260	
$(P_{T,CORE})_1$	11.2	12.4	13.3	13.6	14.0	LBF/IN.^{2}
$(T_{T,CORE})_1$	520	520	520	520	520	^oR

B - Denotes Blockage

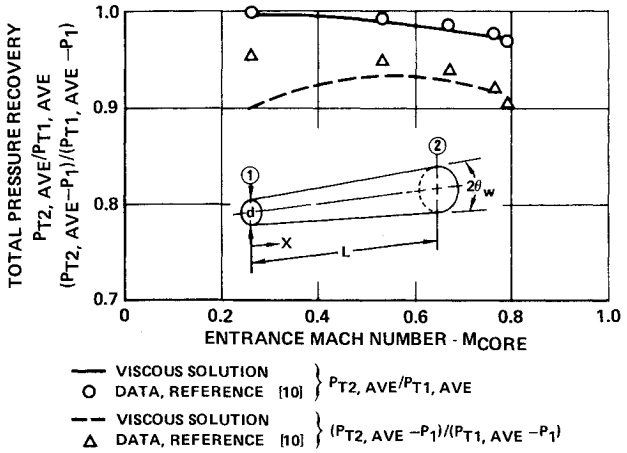

Fig. 7 Effect of diffuser entrance core Mach number on total pressure recovery (conical diffuser with $A_2/A_1=2.0$, $2\theta_w=12°$, and $L/d=2.01$).

DIFFUSER GEOMETRY VARIABLES

COMPLETE DIFFUSER			PLANE-WALL SECTION	
A_3/A_1	L/D	h_1/w_1	A_2/A_1	$2\theta_w$
8	3.5	0.24	2.92	6.80°
8	1.5	0.24	2.92	15.76°
4	3.5	0.48	1.46	3.26°
4	1.5	0.48	1.46	7.60°

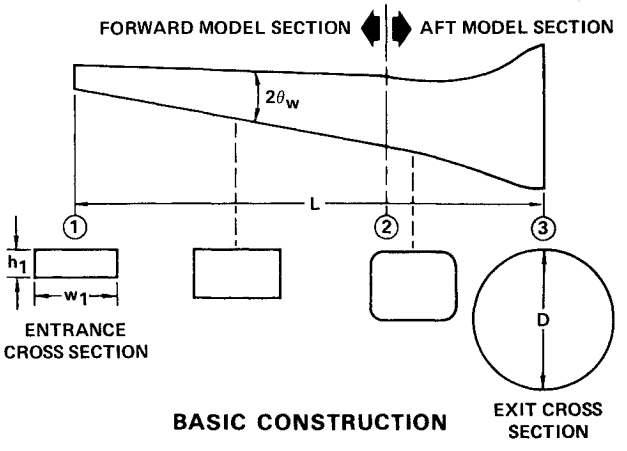

Fig. 8 Construction of subsonic diffuser models with plane-wall section.

analytical and experimental variations of recovery with entrance core Mach number for the diffuser configuration described in Ref. 10. The total pressure recovery is defined in terms of two different parameters. These are $P_{T2,AVE}/P_{TI,AVE}$, which is of interest in propulsion system design, and $(P_{T2,AVE}-P_{WI})/(P_{TI,AVE}-P_{WI})$, which reflects the fraction of the initial difference between the entrance total and static pressure which the diffuser recovers.

Two-Dimensional Diffuser Solutions

Data used to examine the validity of the analytical procedure for two-dimensional diffusers were obtained from a test program conducted by McDonnell Aircraft Co. under contract to the USAF Flight Dynamics Lab.[11] A complete description of the aircraft diffuser models is contained in Ref. 11, but Fig. 8 illustrates, in brief, their construction. The forward section of each diffuser has a constant width and diverging top and bottom plane walls, and the aft section transitions from a rectangular to a circular cross section.

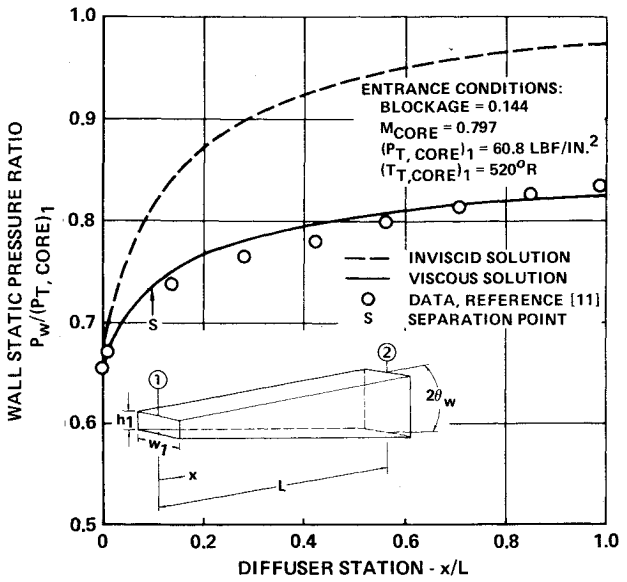

Fig. 9 Comparison of experimental and analytical wall static pressure distributions (plane-wall diffuser with $A_2/A_1=2.92$, $2\theta_w=6.80°$, and $h_1/w_1=0.24$).

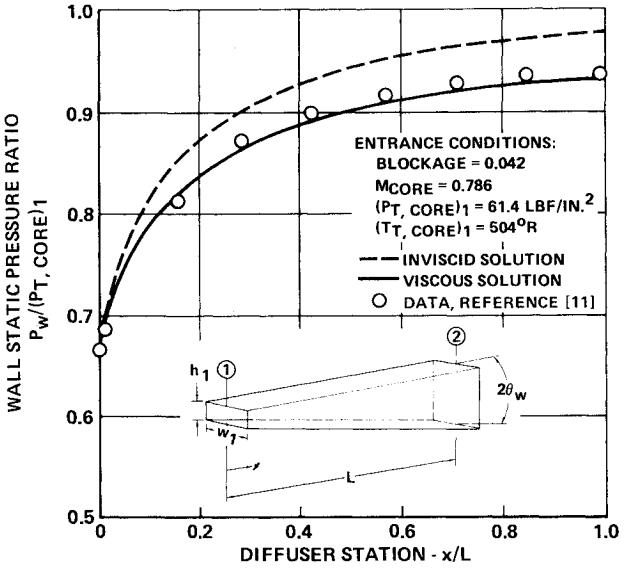

Fig. 10 Comparison of experimental and analytical wall static pressure distributions (plane-wall diffuser with $A_2/A_1=2.92$, $2\theta_w=6.80°$, and $h_1/w_1=0.24$).

The analytical procedure applies directly to the forward portion, which has a rectangular cross section. Figures 9 and 10 show representative distributions of the wall static pressure as ratioed to the core stagnation pressure. As in the examples for the conical diffusers, the inviscid solutions were computed using one-dimensional compressible-flow theory, and the viscous solutions were obtained using the present analytical technique with the entrance conditions listed on each figure. Each solution required approximately one minute of central processing time on a CDC 6600 computer.

According to the analytical model, the diffuser flowfield for the configuration shown in Fig. 9 is separated (an incompressible shape factor of 1.8 or greater is attained), while that shown for the diffuser in Fig. 10 is attached. This is reflected by a flatter distribution in the wall static pressure ratio for the separated diffuser. In the latter case, the pressure

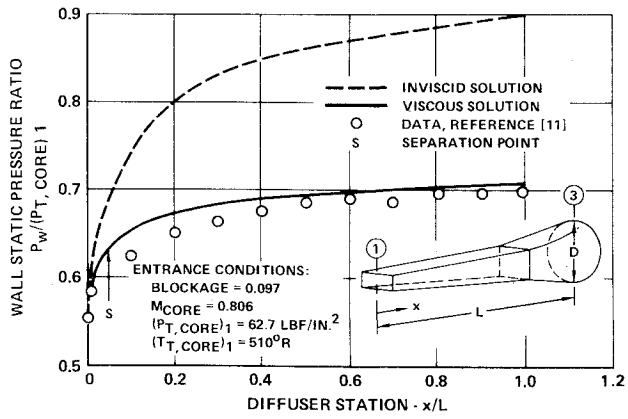

Fig. 11 Comparison of experimental and analytical wall static pressure distributions (plane-wall diffuser transitioning to circular cross section with $A_3/A_1 = 8$, $L/D = 1.5$, and $h_1/w_1 = 0.24$).

TRANSITION TO CIRCULAR CROSS SECTION
ENTRANCE CONDITIONS:

B	0.067	0.097	0.093	0.036	0.097	
M_{CORE}	0.902	0.860	0.736	0.578	0.806	
$(P_{T,CORE})_1$	60.6	62.4	63.0	63.4	62.7	LBF/IN.^{2}
$(T_{T,CORE})_1$	512	511	510	510	510	°R

B — Denotes Blockage

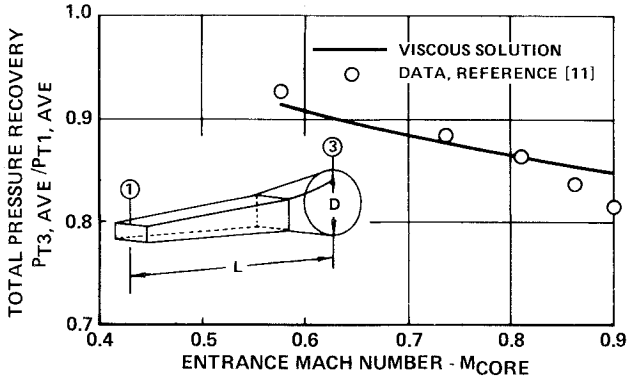

Fig. 12 Effect of diffuser entrance core Mach number on total pressure recovery (plane-wall diffuser transitioning to circular cross section with $A_3/A_1 = 8$, $L/D = 1.5$, and $h_1/w_1 = 0.24$).

ratio more closely follows the form of the inviscid profile, although it is, of course, reduced in magnitude.

The analytical procedure was also applied to the complete diffuser configuration shown in Fig. 8. These diffusers start with a rectangular cross section and transition to a circular one. This geometry cannot be treated directly with the analytical scheme, since the diffuser cross section is neither rectangular nor circular. Therefore, to apply the procedure in an approximate sense, the transition section was treated as an equivalent plane-wall diffuser by taking the width to be constant and computing the height such that the area distributions of the actual and two-dimensional diffusers are the same.

A typical wall static pressure distribution is shown in Fig. 11. Even in the transition, the analytical scheme provides realistic values of the wall static pressure ratio as a function of diffuser station. The explanation for this agreement is the fact that most of the diffusion occurs in the plane-wall section of the duct, and pressure recovery in the transition section is small, regardless of the cross-sectional shape.

Total pressure recovery was also computed for the complete diffuser configurations. The influence of entrance core Mach number on total pressure recovery is shown in Fig. 12. The analytical solution predicts the trend of decreasing recovery with increasing core Mach number that was found in the experimental program described in Ref. 11.

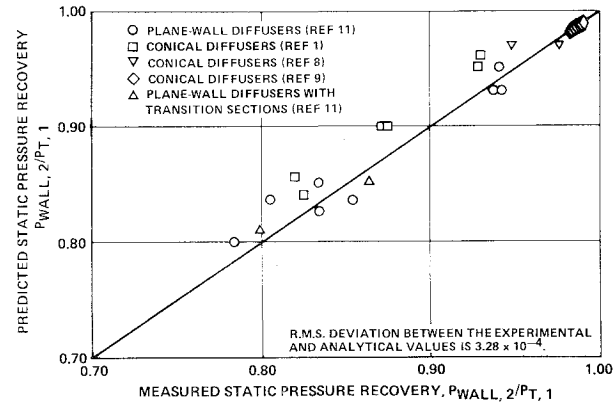

Fig. 13 Comparison of predicted and measured static pressure recovery for three types of diffuser configurations.

Accuracy of Analytical Procedure

The analytical results were compared with experimental results for 25 subsonic diffuser test cases. Figure 13 shows the agreement between the predicted and measured static pressure recovery. The root-mean-square deviation between the experimental and analytical values is 3.28×10^{-4}. The static pressure recovery $P_{W,2}/(P_{T,CORE})_1$ was predicted to within 1% in 54% of the cases, to within 2% in 81% of the cases, and to within 3% in 99% of the cases. The agreement was within 4% for total pressure recovery, $P_{T2,AVE}/P_{T1,AVE}$.

It is postulated that the difference between analytical and experimental results is due primarily to three-dimensional effects. For the conical diffusers, in reality the boundary layer is not axisymmetric, and for the two-dimensional diffusers the boundary layer is not uniform on each wall.

Conclusions

The analytical procedure described here provides a means for predicting the static and total pressure distributions for the attached or separated flow in a subsonic diffuser. The method is directly applicable to the turbulent compressible airflow through ducts with either two-dimensional or axisymmetric cross sections. The following conclusions are drawn with regard to the analytical scheme: 1) The principal advantage of the technique is that it provides a method for evaluating diffuser performance in the presence of separated flow. In addition, it also permits economical computation of diffuser performance when the flow remains attached. 2) In applying the analytical procedure to 25 subsonic diffuser test cases, it was found that the maximum difference between the measured and predicted static pressure recovery is 3%. The greatest deviation between the predicted and measured total pressure recovery was found to be 4%. 3) The usefulness of the analytical procedure can be broadened by extending the analytical model to account for diffuser turning and variable cross section.

References

[1] Means, J.L., Glance, P.C., and Klassen, H.A., "Analytical Investigation of Conical Diffusers," NASA TM X-2065, Aug. 1972.

[2] Reneau, L.R., Johnston, J.P., and Kline, S.J., "Performance and Design of Straight, Two-Dimensional Diffusers," ASME Transactions, *Journal of Basic Engineering, Ser. D,* Vol. 89, March 1967, pp. 141-150.

[3] Klineberg, J.M. and Steger, J.L., "Calculation of Separated Flows at Subsonic and Transonic Speeds," *Third International Conference on Numerical Methods in Fluid Dynamics,* Paris, France, July 3-7, 1972.

[4] Sasman, P.K. and Cresci, R.J., "Compressible Turbulent Boundary Layer with Pressure Gradient and Heat Transfer," *AIAA Journal,* Vol. 4, Jan. 1966, pp. 19-25.

[5]Ludwieg, H. and Tillman, W., "Investigations of the Wall Shearing-Stress in Turbulent Boundary Layers," NACA TN 1285, 1950.

[6]Alber, I.E., "Similar Solutions for a Family of Separated Turbulent Boundary Layers," AIAA Paper 71-203, New York, 1971.

[7]Escudier, M.P. and Nicoll, W.B., "A Shear-Work-Integral Method for the Calculation of Turbulent Boundary-Layer Development," *Proceedings: Computation of Turbulent Boundary Layers-1968, AFOSR-IFP-Stanford Conference,* Vol. I, 1969, pp. 136-146.

[8]Dolan, F.K. and Runstadler, Jr., P.W., "Pressure Recovery Performance of Conical Diffusers at High Subsonic Mach Numbers," Creare TN-165, Jan. 1973, Creare Inc., Hanover, N.H.

[9]Sajben, M., Kroutil, J.C., Sedrick, A.V., and Hoffman, G.H., "Experiments on Conical Diffusers with Distorted Inflow," AIAA Paper 74-529, Palo Alto, Calif.

[10]Little, B.H., Jr. and Wilbur, S.W., "Performance and Boundary Layer Data from 12° and 23° Conical Duffusers of Area Ratio 2.0 at Mach numbers up to Choking and Reynolds Numbers up to 7.5×10^6," NACA Rept. 1201, 1954.

[11]Spong, E.D., Doane, P.M., Rejeske, J.V., and Williams, R.W., "Subsonic Diffuser Designs for Interceptor Applications," Vol. I and II, AFFDL-TR-73-68, June 1973, Wright Patterson Air Force Base, Ohio.